Journal of Translational Medicine

RESEARCH

Open Access

# FGF21 and APOA1 mRNA-based therapies for the treatment of experimental acute pancreatitis

Amaya Lopez-Pascual[1,2], Eva Santamaria[1,3], Nuria Ardaiz[4], Iker Uriarte[1,3], Tiffany Palmer[5], Anne-Renee Graham[5], Celia Gomar[4], Roberto C. Barbero[1,3], M. Ujue Latasa[1,3], Maria Arechederra[1,2,3], Jesus M. Urman[2,6], Carmen Berasain[1,2,3], Antonio Fontanellas[1,2,3], Carlos L. del Rio[5], Maite G. Fernandez-Barrena[1,2,3], Paolo G.V. Martini[5], Joshua R. Schultz[5], Pedro Berraondo[2,4,7*] and Matias A. Avila[1,2,3*]

## Abstract

**Background** Acute pancreatitis (AP) presents a significant clinical challenge with limited therapeutic options. The complex etiology and pathophysiology of AP emphasize the need for innovative treatments. This study explores mRNA-based therapies delivering fibroblast growth factor 21 (FGF21) and apolipoprotein A1 (APOA1), alone and in combination, for treating experimental AP.

**Methods** Liver-targeted lipid nanoparticles (LNP)-mRNA formulations encoding FGF21, APOA1, and a chimeric APOA1-FGF21, were first tested for protein expression and bioavailability in vitro and in mice fed a high-fat diet. Efficacy studies were performed in the caerulein-induced AP (Cer-AP) model, and a new AP model combining ethanol feeding with ethanol binge plus palmitoleic acid administration, the EtOH/POA-AP model. A single dose of the *APOA1*, *FGF21*, and *APOA1-FGF21* LNP-mRNAs formulations was administered in both models. Serum levels of pancreatic lipase (LIPC), amylase (AMYL), and aspartate aminotransferase (AST), along with pancreatic tissue analyses using two histopathological scores were performed to evaluate treatment effects.

**Results** In vitro studies demonstrated the translation and secretion of APOA1, FGF21, and APOA1-FGF21 proteins encoded by the LNP-mRNAs. In vivo, LNP-mRNA administration increased serum levels of the respective proteins in metabolically impaired (i.e. high fat diet-fed) mice. In the Cer-AP model, serum markers of pancreatic injury were similarly reduced when mice were treated with *APOA1*, *FGF21*, and *APOA1-FGF21* LNP-mRNA, and this effect was also observed in the histopathological analyses. The EtOH/POA-AP model was more aggressive than the Cer-AP model. *FGF21* and *APOA1-FGF21* LNP-mRNAs were protective according to LIPC and AMYL serum levels, while *APOA1* LNP-mRNA had little effect. On the other hand, histological improvements were more evident in mice receiving *APOA1* LNP-mRNA. In the EtOH/POA-AP model, *FGF21* and *APOA1-FGF21* LNP-mRNAs reduced serum AST levels, indicating hepatoprotective activity.

*Correspondence:
Pedro Berraondo
pberraondol@unav.es
Matias A. Avila
maavila@unav.es

Full list of author information is available at the end of the article

**Discussion** This proof-of-concept study demonstrates the potential of mRNA-based therapies delivering FGF21 and APOA1 in experimental AP. While individual treatments effectively reduced pancreatic injury, the *APOA1-FGF21* fusion molecule did not exhibit superior activity. Liver-targeted LNP-mRNA administration may offer a promising approach for treating AP, leveraging endogenous production pathways for therapeutic proteins. Further research is warranted to elucidate the mechanisms underlying their therapeutic efficacy and optimize treatment regimens for clinical translation.

**Keywords** Acute pancreatitis, mRNA therapy, FGF21, APOA1, Cytoprotection, Pancreatic injury

## Introduction

Acute pancreatitis (AP), a severe inflammatory disorder of the pancreas, poses a significant clinical challenge, necessitating a deeper understanding of its etiology and pathophysiology to develop therapeutic strategies [1–3]. This acute and potentially life-threatening condition manifests as the sudden inflammation of the pancreatic tissue, with clinical presentations ranging from mild, self-limiting episodes to severe forms associated with systemic complications [3, 4]. In the last decades the global incidence of AP decreased slightly [5], but increased in Western countries, rendering it a growing concern in clinical practice [6]. Moreover, hospitalizations due to AP in countries with high social-demographic indexes (Australasia, North America, and Western Europe) have a better prognosis than those in lower-income countries [5]. Up to date, only moderately effective therapies are available for AP, underscoring the pressing need for innovative therapeutic strategies to address this complex medical condition.

An intricate interplay of genetic and environmental factors contributes to the complexity of this inflammatory condition, necessitating novel therapeutic strategies for effective intervention [2, 7]. The different causes of AP can be easily identified in 75-85% of patients [2]. Current guidelines recommend the identification of the cause of the disease as early as possible, as treatment and follow-up depend on the etiology of pancreatitis [3]. In developed countries, obstruction of the common bile duct by stones (38–45%) and alcohol abuse (20–36%) are the most frequent causes of AP [2, 3, 7]. However, other etiologies should be considered, such as medication, endoscopic retrograde cholangiopancreatography (ERCP), hypercalcemia, hypertriglyceridemia, infection, genetics, autoimmune diseases, excess body weight and (surgical) trauma [3, 8].

Rodents are mostly used to develop models of pancreatitis. In mice and rats, AP in the form of acute inflammation with hemorrhage, when severe, can be induced by injections of caerulein, bile salt infusion, alcohol, duct obstruction, and a choline-deficient ethionine-supplemented (CDE) diet, among others [8–10]. Our study utilizes two distinct mouse models to simulate severe AP: the caerulein-induced model [8, 10, 11] and a novel model induced by a combination of chronic and binge ethanol feeding [12, 13]—established as per the guidelines of the National Institute on Alcohol Abuse and Alcoholism (NIAAA), also called the Gao-binge alcohol model—plus palmitoleic acid (POA, C16:1), a nonoxidative endogenous metabolite of ethanol [14–16]. The selection of these models aligns with the complexity and heterogeneity of AP, enabling a comprehensive evaluation of potential new therapies.

FGF21, known for its anti-inflammatory and metabolic regulatory properties, has been explored in the context of AP therapy [17–19]. These previous studies have paved the way for our investigation into engineered *FGF21* mRNA therapies. On the other hand, reduced serum levels of APOA1, a key component of high-density lipoproteins (HDL), have been associated with inflammation and disease severity in patients with AP [20–24]. Interestingly, recent experimental studies demonstrated a protective role for HDLs and an APOA1-mimetic peptide in AP in vivo models, suggesting potential therapeutic applications [25].

Notably, our work marks the first foray into the application of liver-targeted mRNA-based therapies in the treatment of AP, and introduces an innovative mRNA construct, combining the beneficial elements of both APOA1 and FGF21. Our findings reveal a consistent reduction in inflammation, restoration of pancreatic enzyme levels, and significant improvement in pancreatic histology across all treatments. This collective efficacy underscores the potential synergy between FGF21 and APOA1 in addressing the multifaceted challenges posed by AP.

## Materials and methods

### mRNAs formulation

Codon-optimized mRNAs encoding human *FGF21*, human *APOA1*, and fused human *APOA1-FGF21* mRNA molecules were synthesized in vitro by T7 RNA polymerase-mediated transcription. The mRNAs include a cap, followed by a 5' untranslated region (UTR), an open reading frame (ORF) encoding *FGF21*, *APOA1* or *APOA1*-GS10-*FGF21*, a 3' UTR, and a poly-adenylated tail. Uridine was globally replaced with 1-methylpseudouridine. The constructs used in this study are schematically shown in Fig. 1A. For in vivo delivery, the mRNAs were administered i.v. in LNP formulations prepared as

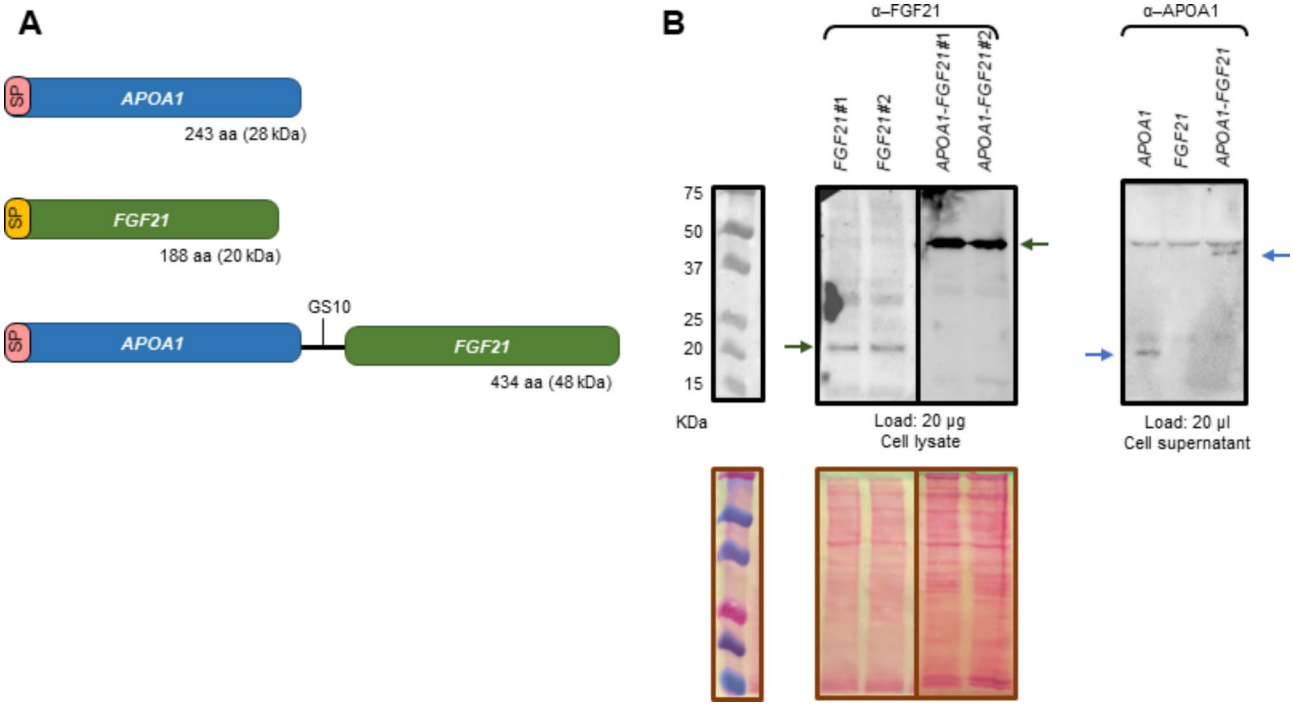


**Fig. 1** *FGF21*, *APOA1*, and fused *APOA1-FGF21* human mRNAs are translated and secreted in mammalian cells. Schematic representation of the different proteins encoded by the tested mRNAs (**A**). HEK293T cells were transfected with 2.5 µg *FGF21*, human *APOA1*, and human fused *APOA1-FGF21* mRNAs, and 24 h later, FGF21 was detected by Western blotting in cell lysates (left blots) and APOA1 in cell culture supernatant (right blot) (**B**). Representative blots are shown. Ponceau staining of membranes is shown to denote equal loading of the gels. SP: signal peptide; GS10: GS linker with 10 amino acids

described [26]. Briefly, mRNA and lipids were mixed at a molar ratio of 3:1 (mRNA/lipid), with lipids composed at a 30:30:38.5:1.5 molar ratio (ionizable lipid/fusogenic lipid/structural lipid/PEG lipid). mRNA-loaded nanoparticles were resuspended in a storage buffer with particle sizes of 80–100 nm, > 80% encapsulation of the mRNA by a RiboGreen assay, and < 10 endotoxin units (EU)/ml. mRNA and LNP were manufactured and provided by Moderna, Inc.

### Cell cultures and reagents

The human embryonic kidney (HEK) 293T cells (ATCC® CRL-3216™) were cultured at 37 °C in a humidified atmosphere containing 5% $CO_2$ in Dulbecco's Modified Eagle Medium (DMEM, Gibco BRL) supplemented with 10% fetal bovine serum (FBS), 2 mM glutamine, and antibiotics (penicillin 100 U/mL and streptomycin 100 µg/mL). Cells seeded at $3 \times 10^5$ in 6-well plates were transfected with 2.5 µg mRNA (*FGF21*, *APOA1*, and *APOA1-FGF21* human mRNA) per well and the TransIT-mRNA transfection reagent. After 24 h, supernatants and cell lysates were harvested for further analysis.

### Animal experiments

For the acute pharmacokinetic in vivo study, 11-week-old C57Bl/6NTac male mice fed with a high-fat diet (HFD) (Research Diets, D12492) for six weeks from Taconic Biosciences (Germantown, NY, USA) were received in our animal facility (CIMA-University of Navarra), where they continued on this diet. Food and water were available *ad libitum*. Upon arrival, mice received an i.p. administration of streptozotocin (STZ) (125 mg/kg). Two weeks later, mice were distributed into LNP-*Control*-mRNA (from now on *Control* [27]), and the LNP-*APOA1*-mRNA, LNP-*FGF21*-mRNA, and LNP-*APOA1-FGF21*-mRNA, treatment groups in a randomized manner based on their body weights. Animals received the LNP-mRNAs (0.5 mg/kg, i.v.), and blood was collected 6, 12, and 24 h after treatments. Mice were sacrificed 24 h after LNP-mRNA administration, and blood was drawn. The liver and epididymal white adipose tissue (eWAT) of these mice were collected to evaluate the effect of the acute LNP-mRNA administrations.

For the efficacy study in AP models, six-week-old C57BL/6JOlaHsd male mice (Envigo, Indianapolis, IN, USA) were received in our animal facility. They were group-housed (4 mice per cage) under standard conditions with *ad libitum* access to water and a standard chow diet.

Caerulein-induced AP (Cer-AP) model: Two weeks after arrival, mice were randomly distributed into the following groups: Tris-sucrose (vehicle), LNP-*Control*-mRNA, LNP-*APOA1*-mRNA and LNP-*APOA1-FGF21*mRNA, each containing 8 mice (except for the

Tris-sucrose group, containing 3 mice). To alleviate signs of pain caused by the severe AP protocol, analgesia was given starting 12 h before and throughout the experiment. Briefly, for a dosage of 1 mg/kg buprenorphine, 0.0094 mg/ml Buprecare (0,3 mg/ml, DFV, Barcelona, Spain) was added to drinking water. On the day of the experiment, mice received seven hourlies intraperitoneal (i.p.) caerulein injections (50 µg/Kg Tocris Bioscience, in 0.9% NaCl), and the Tris-sucrose group received the vehicle (0.9% NaCl). LNP-mRNAs were administered retro-orbitally (0.5 mg/kg, intravenously, i.v.) at the time of the sixth caerulein injection. Tris-sucrose (mRNAs vehicle) was administered retro-orbitally (0.5 mg/kg, i.v.) at the time of the sixth saline injection in the Tris-sucrose group serving as healthy controls. Blood was collected just before the first caerulein/saline injection and after 6, 12, and 24 h. Mice were sacrificed 24 h after the first caerulein/saline injection.

Ethanol/palmitoleic acid-AP (EtOH/POA-AP) model: Two weeks after arriving at our animal facility, mice started the acclimation to the Lieber-DeCarli liquid diet for 3 days. On the first day, mice received a 25% control liquid diet (Rodent Liquid Diet, Lieber-DeCarli 14-726-531 Control Diet Bio-Serv™ F1259SP) and a 75% standard diet. On the second day, mice received a 50% control liquid diet and a 50% standard diet. On the third and last day of acclimation, mice received a 100% control liquid diet. The next day, 3 mice were randomly allocated to the Tris-sucrose (vehicle), and 8 mice were assigned to each one of the LNP-mRNAs groups: LNP-*Control*-mRNA, LNP-*APOA1*-mRNA, LNP-*FGF21*-mRNA, and LNP-*APOA1-FGF21*-mRNA. Animals in the Tris-sucrose group were fed *ad libitum* for 10 days with the control liquid diet, whereas the animals in the LNP-mRNAs groups were fed for 10 days with 5% (vol/vol) ethanol fat-enriched liquid diet (Rodent Liquid Diet, Lieber-DeCarli 14-726-532 Ethanol Diet Bio-Serv™ F1258SP) supplemented with maltose dextrin (Bio-Serv 10DE, ref.3585), as previously described [12, 13]. Mice were offered *ad libitum* access to Lieber-DeCarli Rodent Liquid Diets. The liquid diet was the only source of food and water, and no additional diet or drinking water was provided. Feeding tubes were washed and refilled every day with each freshly prepared diet in the late afternoon, closer to the onset of the dark period of the diurnal cycle, ensuring the availability of diet at the beginning of their maximal food intake period. After the first day of ethanol feeding, the control diet was limited (pair-fed) with the same amount of food consumed by ethanol-fed mice. On the morning of the eleventh day, the mice in the LNP-mRNAs groups received an oral gavage with ethanol (5 g/kg, equivalent to 31.5% vol/vol ethanol solution), and a single i.p. injection of PAO (150 mg/kg in DMSO). The mice in the Tris-sucrose group received an oral gavage of a calorie- and volume-matched maltose dextrin, and an i.p. injection of the vehicle (DMSO). Immediately after the binge and i.p. administration, animals received the LNP-mRNAs retro-orbitally (0.5 mg/kg, i.v.). Blood was collected just before the oral binge and after 6, 12, and 24 h. Mice were sacrificed 24 h after the oral binge.

Blood collected at the specified time points was kept at room temperature for 30 min. The serum and blood cells were separated by centrifugation at 1600xg for 10 min at room temperature. The pancreas was collected at sacrifice and either stored at -80ºC for evaluation for gene expression analyses or collected for formalin-fixed paraffin-embedded (FFPE). The Ethics Committee for Animal Experimentation of the University of Navarra approved all animal studies (protocol #065 – 22).

#### Biochemical parameters

Serum levels of alanine aminotransferase (ALT), aspartate aminotransferase (AST), lipase, and amylase were measured using a C311 Cobas Analyzer (Roche Diagnostics GmbH, Mannheim, Germany) following manufacturer's instructions.

#### ELISAs

The serum concentration of FGF21 and APOA1 after i.v. administration of LNP-mRNAs was determined in serum samples obtained at several time points with a commercial ELISA kit to determine the active moiety (Human FGF21 DuoSet ELISA Kit R&D Systems DY2539, and Human Apolipoprotein A-1 Mabtech ELISA Pro 3710-1HP-2). Serum levels of interleukin 1β (IL-1β) were determined using a commercial ELISA kit (IL-1β/IL-1F2 DuoSet ELISA Kit R&D Systems DY401). All tests were performed according to the manufacturer's instructions.

#### Histological analyses

Mouse pancreatic tissues were fixed in 10% formalin overnight at 4ºC. Paraffin sections were embedded, and preparations were sectioned at 4 µm thickness. Sections from FFPE were stained with hematoxylin-eosin (H&E) for histopathological scoring analysis of the pancreas according to previously described methods [9, 28]. Briefly, based on Schmidt's scoring criteria for pancreas H&E staining, the first and most detailed scoring system published, the degree of pancreatic injury was assessed using a scoring system and grading on an equal weight score (from 0 to 4, average counts per 10 fields at 400x) for edema (expansion: 0 = absent; 0.5-1 = focal-diffuse interlobar septa; 1.5-2 = focal-diffuse interlobular septa; 2.5-3 = focal-diffuse interacinar septa; 3.5-4 = focal-diffuse intercellular spaces), inflammation (inflammation by intralobular or perivascular infiltrate: 0 = 0–1 leukocytes; 0.5 = 2–5 leukocytes: 1 = 6–10 leukocytes; 1.5 = 11–15 leukocytes; 2 = 16–20 leukocytes; 2.5 = 21–25 leukocytes;

3 = 26–30 leukocytes; 3.5 = more than 30 leukocytes or focal microabscesses; 4 = more than 35 leukocytes or confluent microabscesses), acinar necrosis (focal or diffuse necrotic death: 0 = absent; 0.5-1 = focal-diffuse 1–4 necrotic cells; 1.5-2 = focal-diffuse 5–10 necrotic cells; 2.5-3 = focal-diffuse 11–16 necrotic cells; 3.5 = focal occurrence of more than 16 necrotic cells; 4 = extensive confluent necrosis with more than 16 necrotic cells), and a 16-point total severity score (sum of edema, inflammatory infiltrate, and necrosis scores) as previously described [9].

Additionally, we validated the classical histopathological pancreatic score, with a simplified method for the H&E-stained pancreas grading on an equal weight score (0 to 4, 10 fields 400x) for edema (diffuse expansion: 0 = absent; 1 = interlobar septa; 2 = interlobular septa; 3 = interacinar septa; 4 = intercellular spaces), inflammation (inflammatory infiltrate: 0 = 0–5 leukocytes; 1 = 6–15 leukocytes; 2 = 16–25 leukocytes; 3 = 26–35 leukocytes; 4 = more than 36 leukocytes), acinar necrosis (necrotic death: 0 = absent; 1 = 1–4 necrotic cells; 2 = 5–10 necrotic cells; 3 = 11–16 necrotic cells; 4 = more than 16 necrotic cells), and total severity score (sum of edema, inflammatory infiltrate, and necrosis scores, up to 12 points) also as previously described [28]. The whole preparation for each H&E-stained section was analyzed in a blinded fashion, and calculations were made to the size of the equivalence standard scoring system consisting of the average counts per 10 fields at a magnification of 400x. Images were acquired with an Aperio GT 450 DX slide scanner, and automated quantification was performed using the QuPath software v0.4.2.

Immunohistochemical analyses of CD45 and F4/80 positive cells in pancreatic tissues were performed as previously described [29] using the following primary antibodies: ab10558 for CD45 (1:250 dilution) and ab111101 for F4/80 (1:50 dilution), both from Abcam. HRP-conjugated Envision secondary antibody (K4003, DAKO) followed by DAB reagent (K3468, DAKO) were applied for the detection procedure.

### Western blot

As we previously described [30], cell culture samples were homogenized in RIPA lysis buffer (25 mM Tris-HCl pH 7.6, 150 mM NaCl, 1% NP-40, 1% sodium deoxycholate, 0.1% SDS) containing 1x complete protease inhibitor cocktail (Roche). Samples were sonicated for 30 s at maximum intensity with a Bioruptor UCD-200 (Diagenode), then centrifuged at 13,000xg for 20 min at 4 °C, and the supernatants were collected as the whole cell lysates. Protein concentrations were determined using a Pierce BCA Protein Assay Kit (Thermo Fisher Scientific, Waltham, MA, USA). Whole-cell lysates (20 µg/lane) were resolved on a 10% SDS-PAGE gel, and proteins were transferred onto a nitrocellulose membrane (Amersham GE Healthcare, Little Chalfont, UK). Membranes were stained with Ponceau S staining solution (ThermoFisher Scientific) to demonstrate equal loading and then were blocked in 5% skimmed milk (also used for antibody dilution), incubated with α-FGF21 primary antibody (Abcam, ab171941) at 1:1000 and for 1 h in secondary antibody (Anti Rabbit IgG 1:5000 Sigma A0545). For the analysis of cells' conditioned media equal volumes were loaded on gels and membranes were probed with α-APOAI primary antibody (R&D Systems, AF3664) at 1:500 and for 1 h in secondary antibody (Anti Goat IgG 1:5000 Santa Cruz sc-2020). Target antigens were visualized using SuperSignal™ West Pico PLUS chemiluminescent substrate (Thermo Fisher Scientific). Images were scanned with a ChemiDoc Imaging System (Bio-Rad, Hercules, CA, USA) and analyzed using ImageJ software.

### RNA isolation and quantitative reverse transcription PCR (qRT-PCR)

Tissues were mechanically disrupted using a pellet pestle cordless motor in 200 µl of homogenization solution from the simplyRNA Tissue kit (Promega, Madison, WI, USA) and immediately proceeded to RNA extraction with the above-mentioned kit in the automated Maxwell system (Promega). RNA samples (1 µg) were retrotranscribed to cDNA in a thermocycler (1 min at 90 °C for denaturalization followed by 1 h at 37 °C) using a mix containing 50 mM Tris-HCl pH 8.3, 75 mM KCl, and 3 mM $MgCl_2$, 10 ng/µl of random primers, 0.5 mM of each deoxyribonucleic triphosphate (dNTP, Roche Diagnostics, Mannheim, Germany), 5 mM of dithiothreitol (DTT), 1.2 U/µl RNase inhibitors (RNase out) and 6 U/µl of M-MLV reverse transcriptase enzyme. Otherwise stated, all reagents were from Invitrogen (Carlsbad, CA, USA). Quantitative PCR (qPCR) was performed on 25 ng cDNA with iQ SYBR Green Supermix (Bio-Rad) and 0.2 µM of each forward and reverse primer in a CFX96 system, essentially as described [31]. Primer sequences are available upon request. Gene expression was normalized relative to the H3.3 histone A (*H3f3a*) as the housekeeping gene.

### Statistical analyses

For comparing multiple groups to the reference group (AP-induced mice treated with LNP-*Control*-mRNA), one-way ANOVA or the Kruskal-Wallis tests were used according to sample distribution. Multiple comparisons were controlled by the False Discovery Rate (FDR) using the two-stage linear step-up procedure of Benjamini, Krieger, and Yekutieli correction (Q = 5%) GraphPad Prism 9.0.2 software (GraphPad Prism, San Diego, CA, USA) was used for these statistical analyses and the corresponding boxplots. All reported $p$ values were

two-tailed, and differences were considered significant when $p < 0.05$. Where indicated, effect sizes were calculated using Cohen's *d* as described [32] to assess the magnitude of treatment effects in molecular assays. Cohen's *d* values indicate a small (0.2–0.5), medium (0.5–0.8), or large (≥ 0.8) effect, providing a standardized measure of the impact of treatments on molecular studies.

## Results

### Assessment of *FGF21*, *APOA1*, and fusion *APOA1-FGF21* mRNAs expression and biological activity

HEK293T cells were used to test the protein expression of human FGF21, APOA1, and the APOA1-FGF21 fusion from LNP-mRNAs (Fig. 1A). Twenty-four hours post-transfection, cell media was collected, and cells were lysed for Western blot analysis. Lysates were probed with an anti-FGF21 antibody (α-FGF21) (Fig. 1B, left panels). In *FGF21* LNP-mRNAs transfected cells, this antibody detected a band of approximately 20 kDa, corresponding to FGF21. This 20 kDa band was not detected in cells transfected with *APOA1-FGF21* LNP-mRNAs, indicating the specificity of the signal obtained with the α-FGF21 antibody. On the other hand, in these *APOA1-FGF21* LNP-mRNA transfected cells, the α-FGF21 antibody detected a band of approximately 50 kDa, corresponding to the expected size of the fusion APOA1-FGF21 protein. The analysis of supernatants from cells transfected with *APOA1*, *FGF21*, or *APOA1-FGF21* LNP-mRNAs using anti-APOA1 (α-APOA1) antibodies revealed a band of about 28 KDa in samples from cells transfected with *APOA1* LNP-mRNA, corresponding to secreted APOA1 protein (Fig. 1B, right panel). This band was not detected in supernatants from cells transfected with *FGF21* LNP-mRNA, indicating undetectable levels of endogenous APOA1 protein production and the specificity of the signal obtained with the α-APOAI antibody. Finally, a band of approximately 50 kDa was detected with α-APOA1 antibodies in supernatants from cells transfected with *APOA1-FGF21* LNP-mRNA, corresponding to the expected size of the fusion protein (Fig. 1B, right panel). Altogether, these observations demonstrate that the corresponding mRNAs are properly expressed in mammalian cells.

We next tested the in vivo expression of human *FGF21*, *APOA1*, and *APOA1-FGF21* LNP-mRNAs delivered in LNPs to mice treated with STZ and fed with an HFD (H/S mice), to evaluate the protein production and secretion in a model of metabolically impaired and overweight mice. H/S mice received a single dose of human *FGF21*, human *APOA1*, and human *APOA1-FGF21* LNP-mRNAs (0.5 mg/kg, i.v.) and protein levels of APOA1 and FGF21 were analyzed at 12-, and 24-hours post-injections. As shown in Fig. 2A, all LNP-mRNAs were translated, and the corresponding proteins were readily detected in circulation. In agreement with our previous studies on APOA1-fused proteins [30], the stability of APOA1-FGF21 was markedly higher than that of FGF21.

eWAT gene expression in H/S mice 24 h after LNP-mRNAs administration was evaluated. In WAT, *APOA1-FGF21* LNP-mRNA-treated mice showed an increase in *Adipoq* and *Pparg* expression, two FGF21 target genes [33] compared to saline-treated mice (Fig. 2B). The lack of biological response to *FGF21* LNP-mRNA at this timepoint may be attributable to the reduced and less persistent elevation of FGF21 protein levels in serum compared to APOA1-FGF21 (Fig. 2A).

### Effect of *FGF21*, *APOA1*, and *APOA1-FGF21* mRNAs on experimental AP

After testing the functionality of our LNP-mRNA vectors, we implemented two AP models, Cer-AP and EtOH/POA-AP, whose experimental designs are illustrated in Figs. 3A and 4A, to test their efficacy against acute pancreatic damage. First, we validated the expression and secretion of our engineered LNP-mRNAs in the context of these AP models. In the Cer-AP model, serum APOA1 levels increased at 24 h in the *APOA1* and *FGF21-APOA1* mRNA-treated mice (Fig. 3B). Serum FGF21 levels increased at 6-, 12-, and 24 h of AP induction in the *FGF21* and *FGF21-APOA1* mRNA-treated mice (Fig. 3C) in this model. Interestingly, adipose tissue lipolysis leading to the accumulation of circulating free fatty acids and the induction of lipotoxicity has emerged as a pathogenic mechanism in AP, as supported by clinical [34] and experimental observations in the Cer-AP model [35]. On the other hand, the expression of peroxisome proliferator-activated receptor gamma (PPARG) in adipose tissue is known to be induced by increased fat availability [36, 37]. Consistent with all these notions, we found enhanced levels of *Pparg* expression in the adipose tissue of Cer-AP mice, and treatment with *APOA1*, *FGF21*, and *FGF21-APOA1* mRNAs attenuated this response, constituting a preliminary observation that further supports the biological activity of these mRNAs (Supplementary Fig. 1).

In the EtOH/POA-AP model, APOA1 increased at 6-, 12-, and 24 h in the serum of *FGF21-APOA1* LNP-mRNA-treated mice (Fig. 4B). In this model, serum FGF21 increased at 6-, 12-, and 24 h of AP induction in the serum of *FGF21-APOA1* LNP-mRNA-treated mice and at 6 h in the *FGF21* LNP-mRNA-treated mice (Fig. 4C). In summary, the detection of both protein moieties, APOA1 and FGF21, demonstrate higher serum stability of the fusion proteins produced upon administration of *APOA1-FGF21* LNP-mRNA than that observed upon administration of the corresponding *APOA1* or *FGF21* LNP-mRNAs.

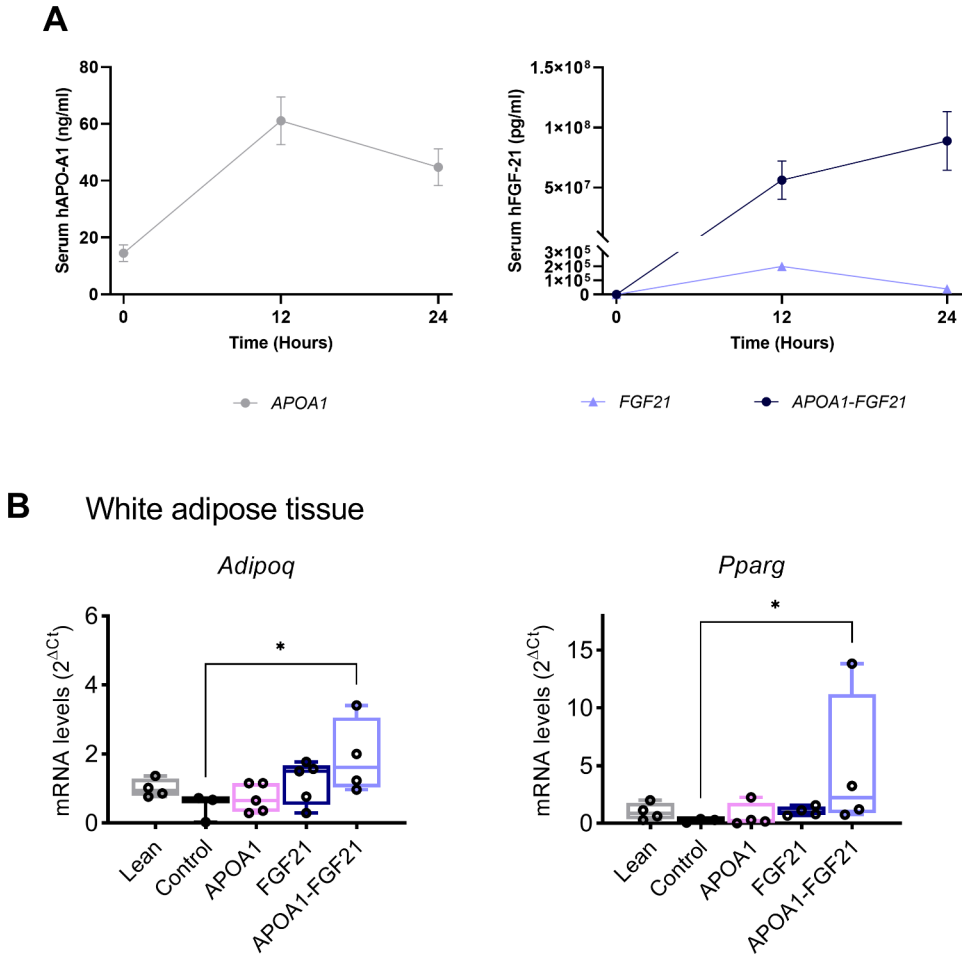


**Fig. 2** Metabolically impaired and overweight mice (H/S mice) administered with a single dose of human *FGF21*, *APOA1*, *APOA1-FGF21* LNP-mRNAs expressed and secreted the corresponding proteins. Evaluation of human APOA1 protein levels in serum from mice after a single administration of human *APOA1* LNP-mRNA, and evaluation of human FGF21 levels in serum from mice after a single administration of *FGF21* or *APOA1-FGF21* LNP-mRNAs at the indicated time-points (**A**). mRNA levels of the indicated genes in the epididymal white adipose tissue from H/S-treated mice 24 h after LNP-mRNAs administration (**B**). *N* = 3 mice in the Lean_Tris-Suc and H/S_Tris-Suc groups, and *n* = 5 in H/S_*APOA1*, H/S_*APOA1-FGF21*, and H/S_*FGF21* groups. A and B: mean and SEM. * *p*-value < 0.05; H/S: high fat-fed and streptozotocin-treated; LNP: lipid nanoparticles; SEM: standard error of the mean

After proving the mRNAs' expression in vivo in the two relevant AP models (Cer-AP and EtOH/POA-AP), we tested the efficacy of these LNP-mRNAs against pancreatic damage in these AP models. Our LNP-mRNAs are targeted to the liver, where the corresponding proteins will be released into circulation [38]. Therefore, first, we tested the serum levels of alanine aminotransferase (ALT) and aspartate aminotransferase (AST) as indicators of potential liver injury. We did not detect significant changes in these parameters among the different treatment groups in the Cer-AP model (Fig. 3D-E). In the EtOH/POA-AP model, while no changes were found in ALT levels, serum AST increased upon EtOH/POA administration in the AP-LNP-*Control*-mRNA group, compared to control mice (Tris-Suc) that did not receive EtOH/POA (Fig. 4D-E). Interestingly, *FGF21* and *APOA1-FGF21* LNP-mRNA treatments were able to reduce serum AST levels, indicating a hepatoprotective activity towards EtOH/POA-induced liver injury (Fig. 4E). Consistent with this hepatoprotective effect, the expression levels of heme oxygenase-1 (*Hmox1*), Mn-superoxide dismutase (*Sod2*) and C-C motif chemokine ligand 2 (*Ccl2*), genes that are upregulated in tissue injury and oxidative stress conditions, tended to be reduced in mice treated with *FGF21* and *APOA1-FGF21* LNP-mRNAs (Supplementary Fig. 2). To quantify the severity of AP, serum amylase (AMYL) and lipase (LIPC) levels were measured. In both AP mouse models, increased serum levels of these markers were found in the vehicle group (LNP-*Control*-mRNA-treated mice) compared to control mice (Tris-Suc) (Figs. 3F-G and 4-F-G). In the Cer-AP model, LIPC was reduced in mice treated with *APOA1* mRNA at 6- and 12 h of AP induction (1- and 7 h after mRNAs administration, respectively), with *FGF21* mRNA at 12 h, and *APOA1-FGF21* mRNA at 6- and 12 h after AP induction (Fig. 3F). AMYL was reduced

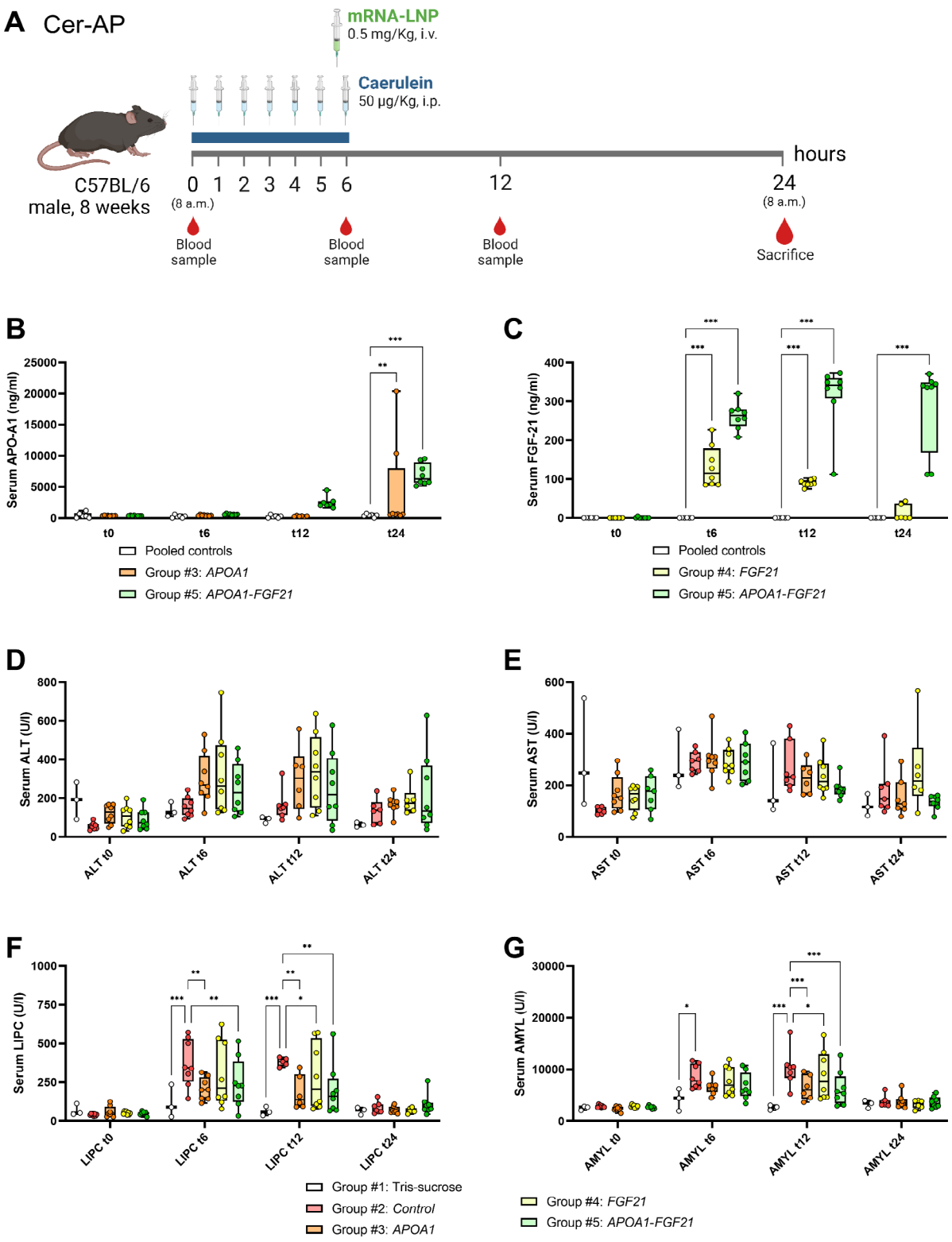


**Fig. 3** Serum markers of AP and liver tissue damage are reduced in the Cer-AP model upon *APOA1*, *FGF21*, and *APOA1-FGF21* LNP-mRNA treatments. Illustration of the experimental setup of Cer-AP model (Created in https://BioRender.com) (**A**). Serum APO-A1 (**B**) and FGF-21 (**C**) levels at 6-, 12-, and 24 h post-induction in the Cer-AP model treated with the LNP-mRNAs. Serum ALT (**D**), AST (**E**), AMYL (**F**), and LIPC (**G**) in Cer-AP-induced mice treated with the LNP-mRNAs. B and C: pooled controls from mice not administered with each molecule; *p*-value * < 0.05, ** < 0.01, *** < 0.001. Cer-AP: caerulein-induced acute pancreatitis; LNP: lipid nanoparticles; ALT: alanine aminotransferase; AST: aspartate aminotransferase; AMYL: amylase; LIPC: lipase

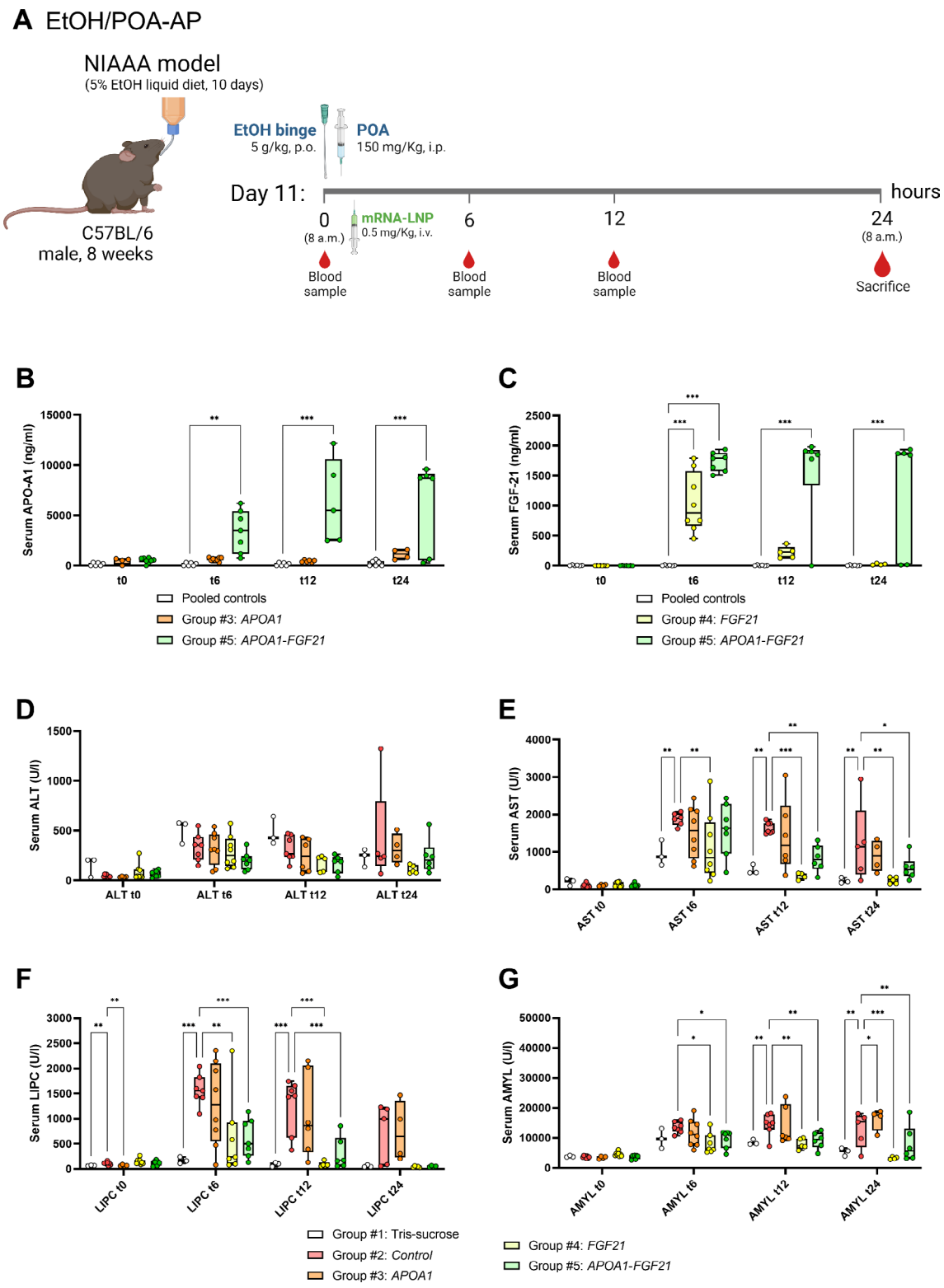


**Fig. 4** Serum markers of AP and liver tissue damage are reduced in the EtOH/POA-AP model upon *APOA1*, *FGF21*, and *APOA1-FGF21* LNP-mRNA treatments. Illustration of the experimental setup of the EtOH/POA-AP model (Created in https://BioRender.com) (**A**). Serum APO-A1 (**B**) and FGF-21 (**C**) levels at 6-, 12-, and 24 h post-induction in the EtOH/POA-AP model treated with the LNP-mRNAs. Serum ALT (**D**), AST (**E**), AMYL (**F**), and LIPC (**G**) in the EtOH/POA-AP-induced mice treated with the LNP-mRNAs. C and D: pooled controls from mice not administered with each molecule; *p*-value * < 0.05, ** < 0.01, *** < 0.001. EtOH/POA-AP: Ethanol/palmitoleic acid-induced acute pancreatitis; LNP: lipid nanoparticles; ALT: alanine aminotransferase; AST: aspartate aminotransferase; AMYL: amylase; LIPC: lipase

by *APOA1*, *FGF21*, and *APOA1-FGF21* mRNAs at 12 h after the Cer-AP induction (Fig. 3G). In the EtOH/POA-AP-induced mice, LIPC was reduced in the *FGF21* and *APOA1-FGF21* mRNAs at 6- and 12 h after AP induction and simultaneous mRNAs administration (Fig. 4F). In this model, AMYL was reduced in the *APOA1* mRNA at 24 h, and by *FGF21*, and *APOA1-FGF21* mRNAs at 6- 12- and 24 h after AP induction and mRNAs administration (Fig. 4G).

#### Administration of *FGF21*, *APOA1*, and *APOA1-FGF21* mRNAs improve histological injury in AP models

To evaluate whether the positive serological effects of LNP-mRNAs correlated with histological improvements, we next examined the pancreatic tissues 24 h after their administration alongside corresponding tissues from control animals. Representative histological images demonstrate an AP phenotype in the Cer-AP and EtOH/POA-AP experimental models (Figs. 5A and 6A). Consistent with previous reports, these AP models showed the histologic macroscopic hallmarks of AP, with increased tissue edema and markedly increased amounts of acinar necrosis and inflammatory foci. In addition, severe AP is evidenced through hemorrhage and fat necrosis. *FGF21*, *APOA1*, and fusion *APOA1-FGF21* LNP-mRNA-treated mice had better appearance and showed less evident edema and inflammation (Figs. 5A and 6A). To quantify pancreatic injury we evaluated pancreas histology using the Schmidt's score [9], which combines parameters of edema, inflammatory infiltrate, necrosis, hemorrhage, and fat necrosis. As expected, the Schmidt's score was markedly increased in both AP models, and in Cer-AP it was reduced in mice treated with *APOA1* and *FGF21* LNP-mRNAs, whereas in the EtOH/POA-AP model *APOA1* LNP-mRNA significantly reduced this score, and *FGF21* and *APOA1-FGF21* LNP-mRNAs showed a trend toward a therapeutic effect ($p$-value = 0.05) (Figs. 5B and 6B). We also validated these effects with a second pancreatic histopathological score with a simplified method scoring for edema, inflammatory infiltrate, and necrosis [28]. This pancreatic injury score was reduced in Cer-AP mice upon treatment with *FGF21*, *APOA1*, and fusion *APOA1-FGF21* LNP-mRNAs (Fig. 5C). In line with these findings, we found that the serum levels of the inflammatory cytokine IL-1β, as well as the pancreatic gene expression of *Hmox1* and insulin-like growth factor-binding protein-1 (*Igfbp1*), known to be upregulated as a reaction to pancreatic injury [25, 39, 40], tended to be reduced by these treatments (Supplementary Fig. 3). These observations are also in agreement with the reduced infiltration of $CD45^+$ cells (lymphocytes) and $F4/80^+$ cells (macrophages) observed in pancreatic tissue sections from mice treated with these three mRNAs (Supplementary Fig. 4). In the EtOH/POA-AP mice the Schmidt's score was only reduced upon *APOA1* LNP-mRNA administration (Fig. 6C). Overall, pancreatic histological evaluation indicated a marked reduction in injury-related parameters comprising pancreatic edema, inflammatory infiltrate, and the extent of necrosis in mice treated with the *FGF21*, *APOA1*, and fusion *APOA1-FGF21* LNP-mRNAs.

## Discussion

AP presents a great challenge in clinical practice due to its substantial morbidity and mortality and the limited therapeutic options, which are mainly restricted to supportive care [1, 41, 42]. Characterized by sudden inflammation of the pancreas with diverse clinical manifestations, AP ranges from mild self-limiting episodes to severe forms with systemic complications [3, 4]. Therefore, there is a pressing need for effective therapeutic approaches to mitigate the multifaceted pathophysiology of the disease and to improve patients' outcomes [5, 6]. Human and experimental AP is characterized by a depletion in pancreatic FGF21, and the recurrent administration of recombinant FGF21 efficiently protected from experimental AP induced by caerulein or ethanol plus POA injection [17]. On the other hand, several studies reported a marked decrease in serum APOA1 levels in association with AP severity and multiple organ failure [20–24]. Importantly, APOA1 has pleiotropic properties that include antioxidant, anti-inflammatory, and cytoprotective effects [43, 44], and a recent report described the protective activity of human HDLs and the repeated injection of an APOA1-mimic peptide in AP models [25]. However, recombinant proteins and peptides have some drawbacks, such as their high production cost, immunogenicity, and generally limited half-life in vivo [38]. In recent years, substantial efforts have been directed toward the development of mRNA therapeutics for the treatment of a variety of metabolic, inflammatory, and neoplastic diseases [45–47]. The innovative potential of mRNAs lies in reduced immune activation, a higher shelf-life, and the use of the individual's body to translate and produce any protein in a relatively sustained manner [38, 48]. In this study, we explored the therapeutic potential of mRNA therapies based on FGF21 and APOA1 in experimental AP. Our pioneering effort testing liver-targeted LNP-mRNAs included a novel APOA1-FGF21 fusion chimera to evaluate if the benefits of both molecules could be harnessed in an additive or synergistic effect mitigating AP.

In our study, we employed two complementary models of AP: the frequently used caerulein model in which transient and mild AP is induced [10], and a new model combining previous approaches based on ten days of ethanol feeding plus a triggering ethanol binge, and a concomitant injection of POA [13, 15], the EtOH/POA model.

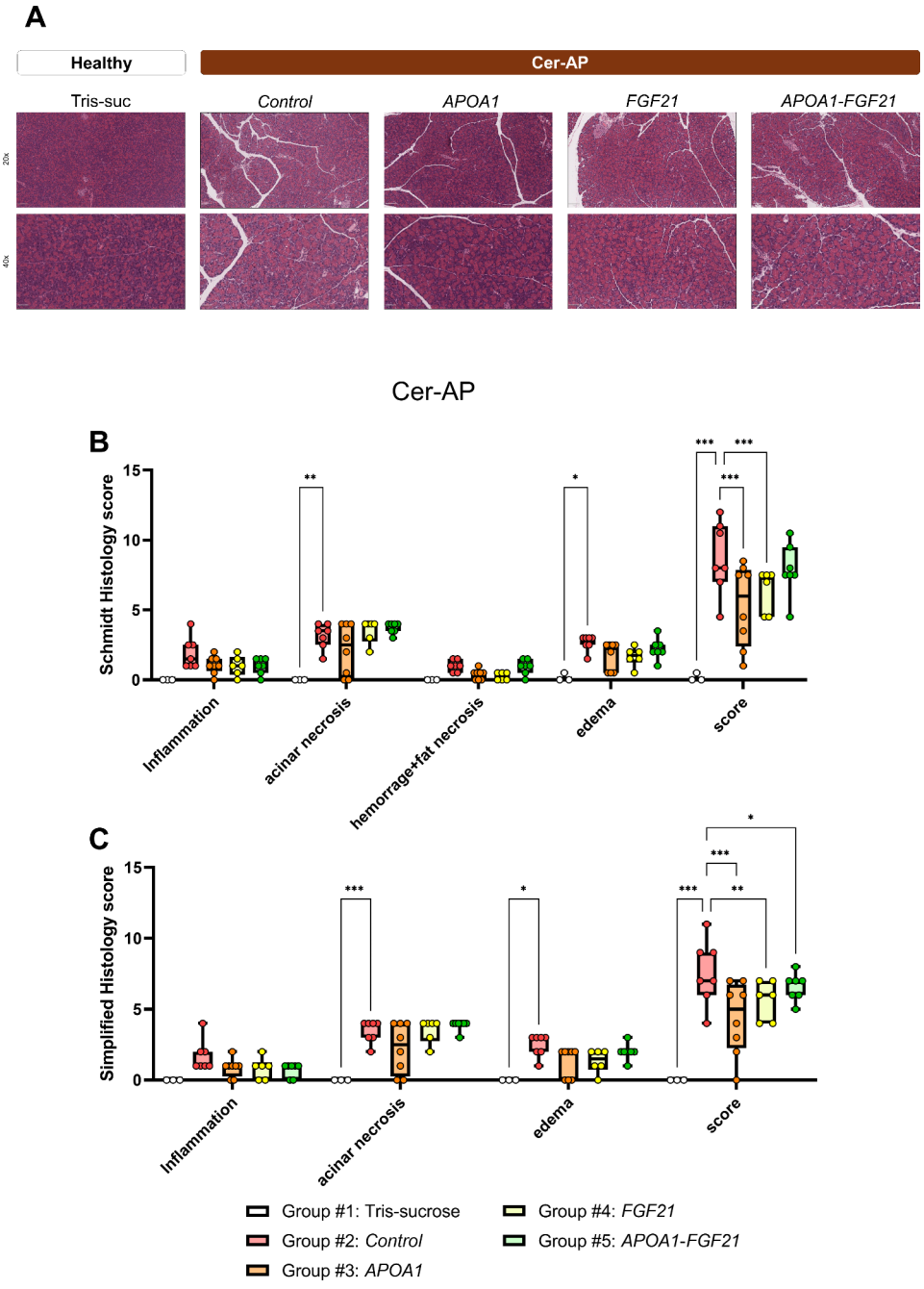


**Fig. 5** Histopathological analyses of pancreatic tissues in the Cer-AP model treated with LNP-mRNAs. Representative images of pancreatic tissues for each model and treatment (H&E, scale bar = 100 µm) (**A**). Histopathological analyses of pancreatic tissues with two pancreatitis scoring systems: Schmidt score (**B**) and a simplified score (**C**) in the Cer-AP model. *p*-value * < 0.05, ** < 0.01, *** < 0.001. Cer-AP: caerulein-induced acute pancreatitis; LNP: lipid nanoparticles; H&E: hematoxylin-eosin

Treatment with *FGF21*, *APOA1*, and *APOA-FGF21* LNP-mRNAs resulted in a similarly significant reversion of AP, as appreciated in the serological and histopathological analyses, indicating that the APOA1-FGF21 chimera does not have superior activity compared to the individual molecules. It is worth noticing that in the recent study demonstrating the protective effects of HDL and an APOA1 mimetic peptide, repeated administrations were given from the first caerulein injection [25], while in our study, a single dose of LNP-mRNAs was administered when mice had already received five caerulein injections, suggesting a better efficacy for our approach. Interestingly, in our LNP-mRNA strategy, the therapeutic proteins are mainly produced in the liver [38], which, together with the intestine, is the natural source of most circulating APOA1 and nascent HDLs [49]. Compared

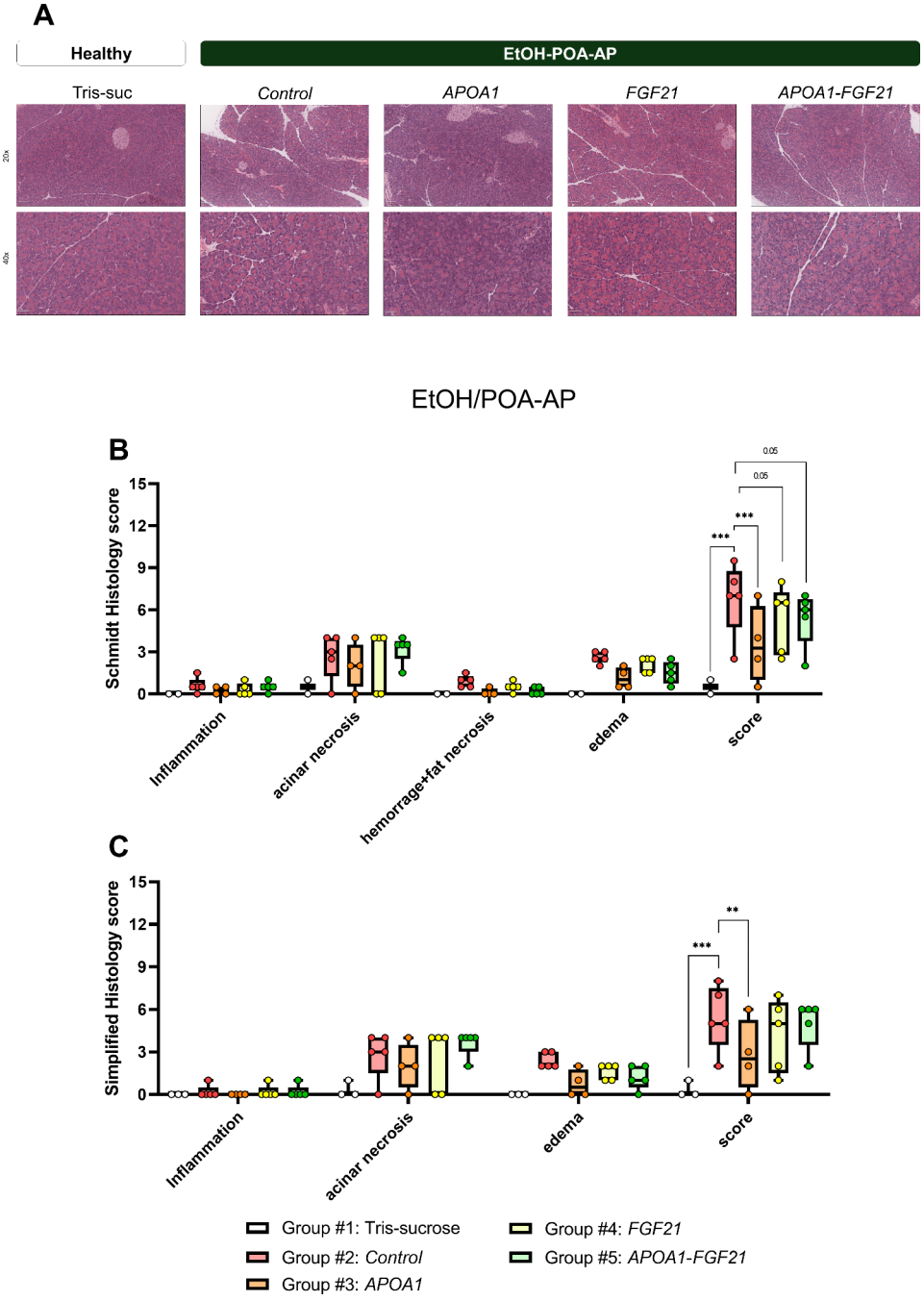


**Fig. 6** Histopathological analyses of pancreatic tissues in the EtOH/POA-AP models treated with LNP-mRNAs. Representative images of pancreatic tissues for each model and treatment (H&E, scale bar = 100 µm) (**A**). Histopathological analyses of pancreatic tissues with two pancreatitis scoring systems: Schmidt score (**B**) and a simplified score (**C**) in the EtOH/POA-AP model. *p*-value * < 0.05, ** < 0.01, *** < 0.001. EtOH/POA-AP: Ethanol/palmitoleic acid-induced acute pancreatitis. LNP: lipid nanoparticles; H&E: hematoxylin-eosin

to the administration of exogenous HDLs, or recombinant APOA1 or APOA1 mimetic peptides, the natural incorporation into HDLs of APOA1 synthesized by the hepatocytes could restore at least in part the constitution and protective function of HDLs, which is known to be altered in inflammatory diseases including AP [23, 25, 49, 50]. This reasoning might also apply to FGF21, for which the liver is the major source of the circulating hormone [51]. The potent and favorable regulatory effects of FGF21 on systemic metabolism have fostered the development and clinical testing of several FGF21 analogs. However, it has become clear that the potency and duration of action of these drugs, including the native recombinant FGF21, greatly differ from the endogenous FGF21

[51]. Therefore, this endogenous and orthotopic production of FGF21 may underlie the significant efficacy of a single LNP-mRNA administration in the Cer-AP model.

In the EtOH/POA-AP model, pancreatic injury is more pronounced and sustained than in the Cer-AP model. POA administration boosts the generation of fatty acids ethyl esters, which are toxic for pancreatic acinar cells and are markedly elevated in patients during alcoholic pancreatitis [52], making it a more clinically relevant model. Interestingly, in this model, we observed that *FGF21* and *APOA1-FGF21* LNP-mRNAs showed protective effects according to serum levels of LIPC and AMYL, while this response was not evident with *APOA1* LNP-mRNA. On the other hand, histological improvements were more evident in mice receiving *APOA1* LNP-mRNA. While at the moment we do not have an explanation for such discrepancy, it could be possible that in this model FGF21 and APOA1-FGF21 mainly have a cytoprotective activity, while APOA1 would contribute more to pancreatic tissue repair (evaluated at the end-point of the study), cosistently with the recently reported effects of an APOA1-mimetic peptide in experimental AP [25]. However, the chimeric molecule would not share this potential reparative activity of APOA1. In patients with AP, the circulating levels of AST are frequently elevated, and some disease scores include this value in the assessment of disease severity [50, 53, 54]. Serum AST levels were also elevated in the EtOH/POA-AP model, and these were significantly reduced by *FGF21* and *APOA1-FGF21* LNP-mRNAs administration. This is an interesting finding suggesting that these treatments could also improve extrapancreatic organ damage in the context of AP. Whether this response depends on the beneficial effects of FGF21 in the pancreatic tissue, or a more direct effect on the liver parenchyma, as endogenous FGF21 has been shown to protect from ethanol-associated liver injury [55], needs to be further elucidated.

## Conclusions

In summary, our findings demonstrate the efficacy of *APOA1* and *FGF21*-based LNP-mRNA therapies in ameliorating pancreatic injury in two distinct mouse models of AP driven by different etiologies (Fig. 7). Importantly, even though we only performed a single administration of our LNP-mRNA formulations, the therapeutic effects were sustained over time, indicating the prolonged efficacy and potential clinical relevance of these therapies in AP management. Nevertheless, it would be interesting to test if this efficacy could be further improved by repeated administrations. The encouraging results of this proof-of-concept study warrant future analyses elucidating the long-term safety and efficacy of these therapies, as well as the characterization of the underlying mechanisms. Finally, although the incidence of AP is higher in men than in women, probably due to the higher prevalence of risk factors for AP, such as smoking, alcohol, abdominal obesity and diabetes [56], and that male sex is associated with higher mortality [57], further studies should evaluate these mRNA-based therapies in AP models implemented in female mice.

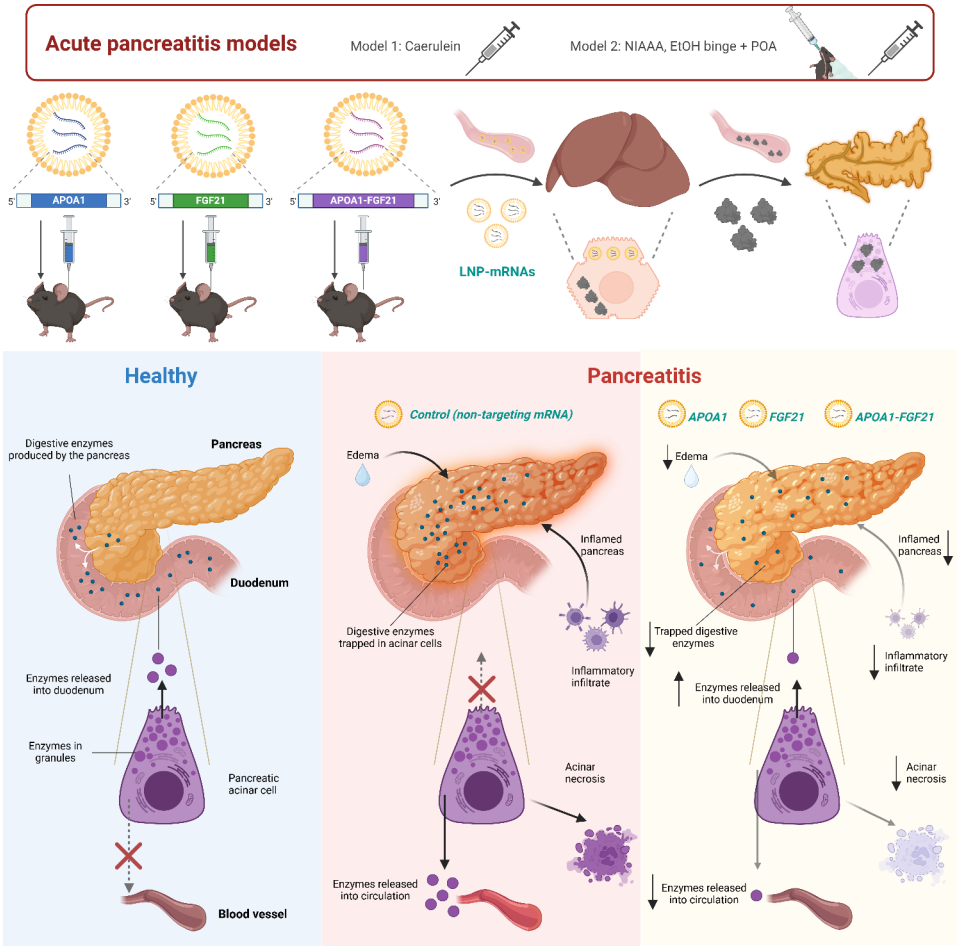


**Fig. 7** Illustration depicting how acute pancreatitis disrupts the normal function of pancreatic acinar cells, which produce digestive enzymes released into the duodenum. Due to several risk factors, acute pancreatitis results in inflammation, edema, and acinar cell necrosis, leading to enzyme leakage into the bloodstream. Two experimental mouse models of acute pancreatitis were treated with LNP-mRNAs encoding APOA1, FGF21, or their fusion chimera. The LNP-mRNAs are targeted to the liver, from where the corresponding proteins will be produced and released into circulation. Treatment reduced inflammation, edema, and necrosis, improved enzyme secretion, and demonstrated prolonged therapeutic effects, suggesting significant potential for these mRNA therapies in managing acute pancreatitis. Created in https://BioRender.com

**Abbreviations**

| | |
|---|---|
| ALT | Alanine aminotransferase |
| AMYL | Amylase |
| AP | Acute pancreatitis |
| APOA1 | Apolipoprotein A1 |
| AST | Aspartate aminotransferase |
| BCA | Bicinchoninic acid |
| CDE | Choline-deficient ethionine-supplemented |
| Cer-AP | Caerulein-induced acute pancreatitis |
| Ccl2 | C-C motif chemokine ligand 2 |
| DMEM | Dulbecco's Modified Eagle Medium |
| dNTP | Deoxyribonucleotide triphosphate |
| DTT | Dithiothreitol |
| ERCP | Endoscopic retrograde cholangiopancreatography |
| EtOH/POA-AP | Ethanol binge plus palmitoleic acid-induced acute pancreatitis |
| EU | Endotoxin units |
| FBS | Fetal bovine serum |
| FDR | False discovery rate |
| FFPE | Formalin-fixed paraffin-embedded |
| FGF21 | Fibroblast growth factor 21 |
| H3f3a | H3.3 histone A |
| H&E | Hematoxylin and eosin |
| H/S | High-Fat Diet and Streptozotocin |
| HDL | High-density lipoprotein |
| HEK | Human embryonic kidney |
| Hmox1 | Heme oxygenase 1 |
| HFD | High-fat diet |
| IL-1β | Interleukin 1β |
| i.p. | Intraperitoneal |
| i.v. | Intravenous |
| Igfbp1 | Insulin-like growth factor-binding protein-1 |
| LIPC | Pancreatic lipase |
| LNP | Lipid nanoparticle |
| NIAAA | National Institute on Alcohol Abuse and Alcoholism |
| ORF | Open reading frame |
| Sod2 | Mn superoxide dismutase |
| POA | Palmitoleic acid |
| STZ | Streptozotocin |
| Tris-Suc | Tris-sucrose |
| UTR | Untranslated region |
| eWAT | Epididymal white adipose tissue |

## Supplementary Information

The online version contains supplementary material available at https://doi.org/10.1186/s12967-025-06129-7.

Supplementary Material 1

Supplementary Material 2

Supplementary Material 3

Supplementary Material 4

Supplementary Material 5

Supplementary Material 6

Supplementary Material 7

**Acknowledgements**
We thank Ms Miriam Belzunce for her excellent technical support. We also thank Mr Eduardo Avila for his generous support.

**Author contributions**
Experiments were designed and supervised by A.L-P., P.B., and M.A.A.; Experimental procedures were carried out by A.L.-P., E.S., N.A., I.U., C.G., R.C.B., and M.U.L. Data curation and interpretation were performed by A.L.-P., M.A., J.U., C.B., A.F., M.G.F.-B., A-R.G., T.P., C.L.R., P.G.V.M., J.R.S., P.B., and M.A.A. Manuscript was written by A.L.-P. and M.A.A. All authors reviewed and approved the final manuscript.

**Funding**
This work was funded in part by Moderna Inc. This study was supported by Instituto de Salud Carlos III (ISCIII) PI22/00147, co-funded by European Union, and Gobierno de Navarra Proyecto ARNMUNE Ref.: 0011–1411-2023-000032 to P.B. M.G.F.-B. receives a Ramón y Cajal Program grant RYC2018-024475-I funded by MCIU/AEI/https://doi.org/10.13039/501100011033 and ESF "Investing in your future". A.L.-P. receives a Sara Borrell Contract CD22/00109 from the Spanish Ministry of Health. M.A. receives a post-doctoral contract POSTD18014AREC from the Asociación Española Contra el Cancer (AECC).

**Data availability**
The data generated during the current study are available within the paper. Any additional information, including further experimental details, is available from the corresponding authors upon reasonable request.

## Declarations

**Ethics approval and consent to participate**
The study received approval from the Ethics Committee for Animal Experimentation of the University of Navarra (protocol #065 – 22).

**Informed consent**
Written informed consent was not applicable.

**Conflict of interest**
Anne-Renee Graham holds stock in and is an employee of Moderna, Inc. The rest of the authors have no conflicts of interest to declare.

**Author details**
[1]Hepatology Laboratory, Solid Tumors Program, CIMA, CCUN, University of Navarra, Pamplona, Spain
[2]Instituto de Investigaciones Sanitarias de Navarra IdiSNA, Pamplona, Spain
[3]CIBERehd, Madrid, Spain
[4]Immunology and Immunotherapy Program, CIMA, CCUN, University of Navarra, Pamplona, Spain
[5]Moderna Inc, Cambridge, MA, USA
[6]Department of Gastroenterology and Hepatology, Navarra University Hospital, Pamplona, Spain
[7]CIBERonc, Madrid, Spain

Received: 14 September 2024 / Accepted: 12 January 2025
Published online: 27 January 2025

**References**

1. Lankisch PG, Apte M, Banks PA, Acute pancreatitis. Lancet. 2015;386:85–96. https://doi.org/10.1016/S0140-6736(14)60649-8.
2. Wang G-J, Gao C-F, Wei D, Wang C, Ding S-Q. Acute pancreatitis: etiology and common pathogenesis. World J Gastroenterol. 2009;15:1427. https://doi.org/10.3748/wjg.15.1427.
3. Boxhoorn L, Voermans RP, Bouwense SA, Bruno MJ, Verdonk RC, Boermeester MA, et al. Acute pancreatitis. Lancet. 2020;396:726–34. https://doi.org/10.1016/S0140-6736(20)31310-6.
4. Banks PA, Bollen TL, Dervenis C, Gooszen HG, Johnson CD, Sarr MG, et al. Classification of acute pancreatitis—2012: revision of the Atlanta classification and definitions by international consensus. Gut. 2013;62:102–11. https://doi.org/10.1136/GUTJNL-2012-302779.
5. Li Cli, Jiang M, Pan Cqiu, Li J, Xu L. gang. The global, regional, and national burden of acute pancreatitis in 204 countries and territories, 1990–2019. BMC Gastroenterol 2021;21:1–12. https://doi.org/10.1186/S12876-021-01906-2/FIGURES/3
6. Iannuzzi JP, King JA, Leong JH, Quan J, Windsor JW, Tanyingoh D, et al. Global incidence of Acute Pancreatitis is increasing over time: a systematic review and Meta-analysis. Gastroenterology. 2022;162:122–34. https://doi.org/10.1053/j.gastro.2021.09.043.
7. Forsmark CE, Swaroop Vege S, Wilcox CM, Acute Pancreatitis. N Engl J Med. 2016;375:1972–81. https://doi.org/10.1056/NEJMra1505202.
8. Lerch MM, Gorelick FS. Models of Acute and Chronic Pancreatitis. Gastroenterology. 2013;144:1180–93. https://doi.org/10.1053/j.gastro.2012.12.043.
9. Schmidt J, Rattner DW, Lewandrowski K, Compton CC, Mandavilli U, Knoefel WT, et al. A Better Model of Acute Pancreatitis for evaluating therapy. Ann Surg. 1992;215:44–56. https://doi.org/10.1097/00000658-199201000-00007.
10. Silva-Vaz P, Abrantes AM, Castelo-Branco M, Gouveia A, Botelho MF, Tralhão JG. Murine models of Acute Pancreatitis: a critical Appraisal of Clinical Relevance. Int J Mol Sci. 2019;20:2794. https://doi.org/10.3390/ijms20112794.
11. Su KH, Cuthbertson C, Christophi C. Review of experimental animal models of acute pancreatitis. HPB. 2006;8:264–86. https://doi.org/10.1080/13651820500467358.
12. Bertola A, Mathews S, Ki SH, Wang H, Gao B. Mouse model of chronic and binge ethanol feeding (the NIAAA model). Nat Protoc. 2013;8:627–37. https://doi.org/10.1038/nprot.2013.032.
13. Wang S, Ni H-M, Chao X, Ma X, Kolodecik T, De Lisle R, et al. Critical role of TFEB-Mediated lysosomal Biogenesis in Alcohol-Induced Pancreatitis in mice and humans. Cell Mol Gastroenterol Hepatol. 2020;10:59–81. https://doi.org/10.1016/j.jcmgh.2020.01.008.
14. He Y, Dai J, Niu M, Li B, Chen C, Jiang M, et al. Inhibition of nicotinamide phosphoribosyltransferase protects against acute pancreatitis via modulating macrophage polarization and its related metabolites. Pancreatology. 2021;21:870–83. https://doi.org/10.1016/j.pan.2021.03.011.
15. Huang W, Booth DM, Cane MC, Chvanov M, Javed MA, Elliott VL, et al. Fatty acid ethyl ester synthase inhibition ameliorates ethanol-induced ca 2+ -dependent mitochondrial dysfunction and acute pancreatitis. Gut. 2014;63:1313–24. https://doi.org/10.1136/gutjnl-2012-304058.
16. Vigna SR, Shahid RA, Liddle RA. Ethanol contributes to neurogenic pancreatitis by activation of TRPV1. FASEB J. 2014;28:891–6. https://doi.org/10.1096/fj.13-236208.
17. Hernandez G, Luo T, Javed TA, Wen L, Kalwat MA, Vale K, et al. Pancreatitis is an FGF21-deficient state that is corrected by replacement therapy. Sci Transl Med. 2020;12:5186. https://doi.org/10.1126/scitranslmed.aay5186.
18. Johnson CL, Weston JY, Chadi SA, Fazio EN, Huff MW, Kharitonenkov A, et al. Fibroblast growth factor 21 reduces the severity of Cerulein-Induced Pancreatitis in mice. Gastroenterology. 2009;137:1795–804. https://doi.org/10.1053/j.gastro.2009.07.064.
19. Chen Q, Li J, Ma J, Yang X, Ni M, Zhang Y, et al. Fibroblast growth factor 21 alleviates acute pancreatitis via activation of the Sirt1-autophagy signalling pathway. J Cell Mol Med. 2020;24:5341–51. https://doi.org/10.1111/jcmm.15190.
20. Li Y, Zheng R, Gao F, Wang L, Feng S, Li J, et al. Association between high-density lipoprotein cholesterol and apolipoprotein A-I and severe acute pancreatitis: a case-control study. Eur J Gastroenterol Hepatol. 2021;33:1517–23. https://doi.org/10.1097/MEG.0000000000002095.
21. Yin Y, Wei N, Zheng Z, Liang H. Relationship between apoA-I, chemerin, Procalcitonin and severity of hyperlipidaemia-induced acute pancreatitis. J Pak Med Assoc. 2022;72:1201–4. https://doi.org/10.47391/JPMA.3700.
22. Wu J, Wang Y, Li H, Tan W, Chen X, Ye S. Serum apolipoprotein B-to-apolipoprotein A1 ratio is independently associated with disease severity in patients

with acute pancreatitis. Sci Rep. 2019;9:7764. https://doi.org/10.1038/s41598-019-44244-w.
23. Yu G, Jiang W, Cheng Z, Wan R. Predictive value of serum apolipoprotein A-I in the organ failure of acute pancreatitis: a retrospective cohort study. Scand J Gastroenterol. 2023;58:1049–55. https://doi.org/10.1080/00365521.2023.2200500.
24. Hu YQ, Tao X, Wu HB, Li WG, Chen DY, Liu YF, et al. Predicting Severity in Hypertriglyceridemia-Induced Acute Pancreatitis: the role of neutrophils, calcium, and apolipoproteins. Med Sci Monit. 2024;30. https://doi.org/10.12659/MSM.942832.
25. Lu Y, Li B, Wei M, Zhu Q, Gao L, Ma N, et al. HDL inhibits pancreatic acinar cell NLRP3 inflammasome activation and protect against acinar cell pyroptosis in acute pancreatitis. Int Immunopharmacol. 2023;125. https://doi.org/10.1016/J.INTIMP.2023.110950.
26. Cornebise M, Narayanan, Elisabeth, Xia, Yan, Acosta, Edward, Ci, Lei, Koch, Hillary, Milton, Jaclyn, Sabnis, Staci, Salerno, Timothy BKE. Discovery of a Novel Amino Lipid That Improves Lipid Nanoparticle Performance through Specific Interactions with mRNA. Adv Funct Mater. 2021;2106727.
27. Lopez-Pascual A, Russo-Cabrera JS, Ardaiz N, Palmer T, Graham A-R, Uriarte I, et al. Non-mitogenic FGF19 mRNA-based therapy for the treatment of experimental metabolic dysfunction-associated steatotic liver disease (MASLD). Clin Sci. 2024;138:1265–84. https://doi.org/10.1042/CS20241137.
28. Liu X, Zhu Q, Zhang M, Yin T, Xu R, Xiao W, et al. Isoliquiritigenin ameliorates Acute Pancreatitis in mice via inhibition of oxidative stress and modulation of the Nrf2/HO-1 pathway. Oxid Med Cell Longev. 2018;2018:1–12. https://doi.org/10.1155/2018/7161592.
29. Elurbide J, Colyn L, Latasa MU, Uriarte I, Mariani S, Lopez-Pascual A, et al. Identification of PRMT5 as a therapeutic target in cholangiocarcinoma. Gut. 2024;0:1–12. https://doi.org/10.1136/gutjnl-2024-332998.
30. Alvarez-Sola G, Uriarte I, Latasa MU, Fernandez-Barrena MG, Urtasun R, Elizalde M, et al. Fibroblast growth factor 15/19 (FGF15/19) protects from diet-induced hepatic steatosis: development of an FGF19-based chimeric molecule to promote fatty liver regeneration. Gut. 2017;66:1818–28. https://doi.org/10.1136/gutjnl-2016-312975.
31. Barcena-Varela M, Paish H, Alvarez L, Uriarte I, Latasa MU, Santamaria E, et al. Epigenetic mechanisms and metabolic reprogramming in fibrogenesis: dual targeting of G9a and DNMT1 for the inhibition of liver fibrosis. Gut. 2020;70(gutjnl–2019–320205). https://doi.org/10.1136/gutjnl-2019-320205.
32. Cohen J. Statistical Power Analysis for the behavioral sciences. Stat Power Anal Behav Sci. 2013. https://doi.org/10.4324/9780203771587.
33. Dutchak PA, Katafuchi T, Bookout AL, Choi JH, Yu RT, Mangelsdorf DJ, et al. Fibroblast growth Factor-21 regulates PPARγ activity and the antidiabetic actions of thiazolidinediones. Cell. 2012;148:556. https://doi.org/10.1016/J.CELL.2011.11.062.
34. Tian Y, Huang Q, Ren YT, Jiang X, Jiang B. Visceral adipose tissue predicts severity and prognosis of acute pancreatitis in obese patients. Hepatobiliary Pancreat Dis Int. 2024;23:458–62. https://doi.org/10.1016/J.HBPD.2023.08.014.
35. Xie X, Liu Y, Yang Q, Ma X, Lu Y, Hu Y, et al. Adipose triglyceride lipase-mediated adipocyte lipolysis exacerbates Acute Pancreatitis Severity in Mouse models and patients. Am J Pathol. 2024;194:1494–510. https://doi.org/10.1016/J.AJPATH.2024.03.014.
36. Kang K, Liu W, Albright KJ, Park Y, Pariza MW. trans-10,cis-12 CLA inhibits differentiation of 3T3-L1 adipocytes and decreases PPARγ expression. Biochem Biophys Res Commun. 2003;303:795–9. https://doi.org/10.1016/S0006-291X(03)00413-3.
37. Desvergne B, Wahli W. Peroxisome proliferator-activated receptors: nuclear control of metabolism. Endocr Rev. 1999;20:649–88. https://doi.org/10.1210/EDRV.20.5.0380.
38. Berraondo P, Martini PGVV, Avila MA, Fontanellas A. Messenger RNA therapy for rare genetic metabolic diseases. Gut. 2019;68:1323–30. https://doi.org/10.1136/gutjnl-2019-318269.
39. Lu J, Liu K, Schulz N, Karampelias C, Charbord J, Hilding A, et al. IGFBP1 increases β-cell regeneration by promoting α- to β-cell transdifferentiation. EMBO J. 2016;35:2026–44. https://doi.org/10.15252/EMBJ.201592903.
40. Karna E, Surazynski A, Orłowski K, Łaszkiewicz J, Puchalski Z, Nawrat P, et al. Serum and tissue level of insulin-like growth factor-I (IGF-I) and IGF-I binding proteins as an index of pancreatitis and pancreatic cancer. Int J Exp Pathol. 2002;83:239–46. https://doi.org/10.1046/J.1365-2613.2002.00237.X.
41. Van Dijk SM, Hallensleben NDL, Van Santvoort HC, Fockens P, Van Goor H, Bruno MJ, et al. Acute pancreatitis: recent advances through randomised trials. Gut. 2017;66:2024–32. https://doi.org/10.1136/GUTJNL-2016-313595.
42. Peery AF, Crockett SD, Murphy CC, Jensen ET, Kim HP, Egberg MD, et al. Burden and cost of gastrointestinal, liver, and pancreatic diseases in the United States: Update 2021. Gastroenterology. 2022;162:621–44. https://doi.org/10.1053/J.GASTRO.2021.10.017.
43. Jackson AO, Rahman GA, Long S. Apolipoprotein-AI and AIBP synergetic anti-inflammation as vascular diseases therapy: the new perspective. Mol Cell Biochem. 2021;476:3065–78. https://doi.org/10.1007/S11010-020-04037-6.
44. Cochran BJ, Ong KL, Manandhar B, Rye KA. APOA1: a protein with multiple therapeutic functions. Curr Atheroscler Rep. 2021;23. https://doi.org/10.1007/S11883-021-00906-7.
45. Cacicedo ML, Limeres MJ, Gehring S. mRNA-Based approaches to treating Liver diseases. Cells. 2022;11. https://doi.org/10.3390/CELLS11203328.
46. Córdoba KM, Jericó D, Sampedro A, Jiang L, Iraburu MJ, Martini PGV, et al. Messenger RNA as a personalized therapy: the moment of truth for rare metabolic diseases. Volume 372, 1st ed. Elsevier Inc.; 2022. https://doi.org/10.1016/bs.ircmb.2022.03.005.
47. Rohner E, Yang R, Foo KS, Goedel A, Chien KR. Unlocking the promise of mRNA therapeutics. Nat Biotechnol. 2022;40:1586–600. https://doi.org/10.1038/S41587-022-01491-Z.
48. Wang YS, Kumari M, Chen GH, Hong MH, Yuan JPY, Tsai JL, et al. mRNA-based vaccines and therapeutics: an in-depth survey of current and upcoming clinical applications. J Biomed Sci 2023. 2023;301:30:1–35. https://doi.org/10.1186/S12929-023-00977-5.
49. Morris G, Puri BK, Bortolasci CC, Carvalho A, Berk M, Walder K, et al. The role of high-density lipoprotein cholesterol, apolipoprotein A and paraoxonase-1 in the pathophysiology of neuroprogressive disorders. Neurosci Biobehav Rev. 2021;125:244–63. https://doi.org/10.1016/J.NEUBIOREV.2021.02.037.
50. Bugdaci MS, Sokmen M, Zuhur SS, Altuntas Y. Lipid profile changes and importance of low serum α-lipoprotein fraction (high-density lipoprotein) in cases with acute pancreatitis. Pancreas. 2011;40:1241–4. https://doi.org/10.1097/MPA.0B013E3182211BBF.
51. Kliewer SA, Mangelsdorf DJ. A Dozen years of Discovery: insights into the physiology and pharmacology of FGF21. Cell Metab. 2019;29:246–53. https://doi.org/10.1016/J.CMET.2019.01.004.
52. Vela S, Guerra A, Farrell G, Trivedi S, Chaffin H, Rood C, et al. Pathophysiology and biomarker potential of fatty acid Ethyl Ester Elevation during alcoholic pancreatitis. Gastroenterology. 2021;161:1513–25. https://doi.org/10.1053/J.GASTRO.2021.07.029.
53. Mederos MA, Reber HA, Girgis MD, Acute Pancreatitis. Rev JAMA. 2021;325:382–90. https://doi.org/10.1001/JAMA.2020.20317.
54. Xu F, Hu X, Li S. Exploring the value of early laboratory indicators combined with pancreatitis activity scoring system in assessing the severity and prognosis of acute pancreatitis. Pakistan J Med Sci. 2023;39. https://doi.org/10.12669/PJMS.39.5.7543.
55. Desai BN, Singhal G, Watanabe M, Stevanovic D, Lundasen T, Fisher ffolliott M, et al. Fibroblast growth factor 21 (FGF21) is robustly induced by ethanol and has a protective role in ethanol associated liver injury. Mol Metab. 2017;6:1395–406. https://doi.org/10.1016/J.MOLMET.2017.08.004.
56. Wang M, Gorelick F, Bhargava A. Sex differences in the exocrine pancreas and Associated diseases. Cell Mol Gastroenterol Hepatol. 2021;12:427–41. https://doi.org/10.1016/J.JCMGH.2021.04.005.
57. Drake M, Dodwad SJM, Davis J, Kao LS, Cao Y, Ko TC. Sex-related differences of Acute and chronic pancreatitis in adults. J Clin Med. 2021;10:1–11. https://doi.org/10.3390/JCM10020300.

## Publisher's note